

Followstopper Revisited: Phase-space Lagrangian Controller for Traffic Decongestion

Rahul Bhadani

Electrical and Computer Engineering

The University of Alabama in Huntsville, Huntsville, AL, USA

Email: rahul.bhadani@uah.edu

June 11, 2025

Abstract

This paper revisits Followstopper, a phase-space-based control system that had demonstrated its ability to mitigate emergent traffic jams due to stop-and-go traffic during rush hour in the mixed-autonomy setting. Followstopper was deployed on an autonomous vehicle. The controller attenuates the emanant traffic waves by regulating its velocity according to the relative distance and velocity of the leader car. While regulating the velocity, the controller also prevents the collision of the ego vehicle with the lead vehicle within the range specified by the controller's design parameter. The controller design is based on a configurable quadratic curve on relative distance-relative velocity phase-space that allows the transition of the regulated velocity from (i) no modification of input, (ii) decelerating to match the leader's velocity (iii) braking to avoid any imminent collision. In this paper, we explore the phase-space properties of Followstopper and provide a detailed description of a nonlinear control law that regulates the reference input to Followstopper within the physics-informed boundaries. We also provide a new discussion on the nominal control law that regulates the reference speed to Followstopper to avoid unrealistic and unsafe acceleration.

1 Introduction

Several analyses [1–3] of available data provided by the government and private agencies such as the Bureau of Public Roads show that cities are increasingly crossing new limits on road capacity. In the interest of solving the traffic congestion problem in an urban area, researchers from all around the world proposed several models to understand traffic dynamics [4–7]. Several car-following models [8–12] were proposed to understand how consumer cars interact in traffic. Following the rich understanding of car-following models and traffic dynamics, Yuki Sugiyama and his team [13] demonstrated that traffic congestion emerges without an infrastructure bottleneck when road capacity exceeds the limit, resulting in traffic waves. With the advent of new vehicle technologies such as Adaptive Cruise Control (ACC), intelligent driver-assisted systems, cooperative driving, and autonomous vehicles (AVs), it

is considered that intelligent vehicles will be able to alleviate the problems arising from increasingly congested urban road networks [14]. As the share of level 5 autonomous vehicles is not expected to reach 100% for a few years, AVs will have to operate in mixed traffic composed of vehicles at various levels of automation, ranging from fully manual driving to level 5.

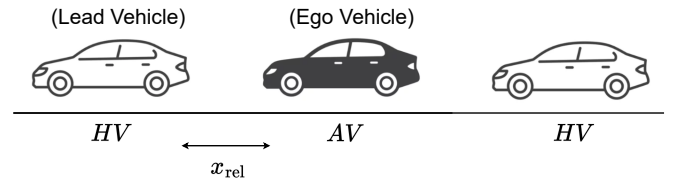


Figure 1: An autonomous vehicle following a human-driven vehicle, which is in turn followed by another human-driven vehicle.

Since the seminal Arizona Ring-road Experiment [15] that demonstrated the capability of a highly automated vehicle to dissipate phantom traffic jams, the research on traffic decongestion controllers has exploded dramatically. Since the inception, methods of traffic decongestion controller have emerged such as optimal control [16] where authors analyze the controllability and stabilizable of a ring-road mixed traffic, model-predictive control [17] where authors adopt point-mass model for the dynamics of an autonomous vehicle (AV) to be controlled for traffic decongestion, and human-driven vehicle (HV) using intelligent driver model (IDM) with a sequence of interaction between them. In [18], authors consider the scenario of platooning with inter-vehicle communication between vehicles that is controlled by a cellular automaton model and a safe distance model. In [19], the authors presented a benchmark for testing the impact of traffic decongestion using a reinforcement learning based AV controller. In [20], authors developed a deep reinforcement learning based AV controller to optimize fuel consumption and reduce traffic congestion simultaneously in a mixed-autonomy traffic. In another work [21], authors used imitation learning for creating a traffic decongestion controller in a mixed-autonomy scenario. However, all of these subsequent works have been on the simulation studies and at the same time neglect practical engineering challenges such as data acquisi-

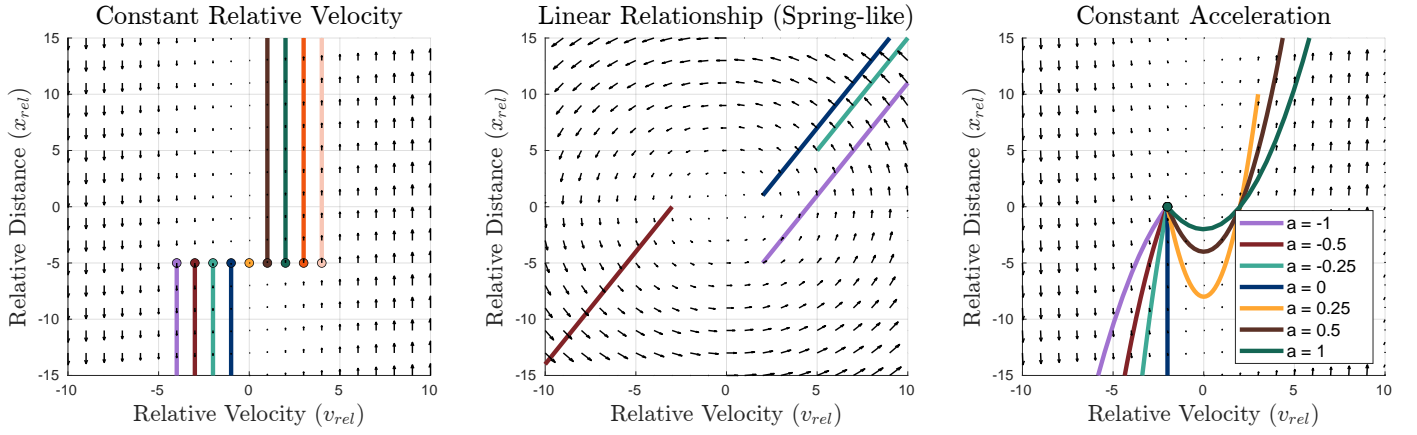


Figure 2: Phase-Space Portraits for Three Dynamical Systems Categories for Two-Car-Following Systems

tion, real-world vehicle dynamics, and external disturbances while modeling the controller as well as the human driver.

In contrast to traditional Eulerian highway traffic controls (such as ramp metering, variable speed limits, traffic lights), traffic control via autonomous vehicle control is called Lagrangian control, where autonomous vehicles act as mobile actuators. The successful demonstration of the Lagrangian phase-space controller in Tucson, Arizona, in December 2016 [15], required the design of a control strategy and significant innovation in terms of real-time data processing and filtering to handle heterogeneous in-vehicle sensor networks. However, the discussion on the prior work lacked significant discussion on the mathematical formulation of the phase-space approach that led to the design of Followerstopper. In addition, the nominal controller that regulates the reference speed of Followerstopper has not been discussed in the literature.

1.1 Contribution

The contribution of this paper is towards discussing the background on phase-space-based non-linear control techniques that were used for the mitigation of traffic waves by deploying an autonomous vehicle as a Lagrangian actuator. The controller should be able to change the velocity of the autonomous vehicle smoothly from the reference velocity. The reference velocity is the velocity at which the flow dynamics of the traffic are expected to be stable. Such reference velocity comes either from an expert or from a nominal controller. We provide further discussion of the nominal control algorithm that is currently absent in the literature. The required controller is named *Followerstopper* controller, a controller that maintains a reference velocity in the flow (*follower*) but can avoid the need to execute collision avoidance style braking (*stopper*), since an underlying assumption of the flow dynamics is that the lead vehicle may be either speeding up or slowing down, as the AV approaches. The idea behind such a design is a controller with switching modes such that the acceleration profile does not result in further traffic wave propagation for some mode and mitigates traffic waves for some other

modes. Such a design uses phase-space techniques for specifying various modes that are discussed in detail in the forthcoming section.

2 Mixed-Autonomy Traffic Scenario

A typical scenario in the mixed traffic where a Lagrangian control vehicle (ego vehicle) follows a human-driven vehicle, as deployed in the Arizona ring-road experiment [15], is shown in Figure 1. Typically, an ego vehicle is an autonomous vehicle (AV) or an adaptive cruise control vehicle (ACC).

To describe the experimental setup, we use the following notation for this paper:

- $x_{\text{rel}} : [0, \infty) \rightarrow \mathbb{R}$: relative distance between the leading vehicle and the ego vehicle;
- $v_{\text{lead}} : [0, \infty) \rightarrow \mathbb{R}$: leading vehicle speed;
- $v_{\text{AV}} : [0, \infty) \rightarrow \mathbb{R}$: ego (AV) speed;
- $v_{\text{rel}} : [0, \infty) \rightarrow \mathbb{R}$: relative speed between the leading vehicle and the ego vehicle, specifically $v_{\text{rel}} = v_{\text{lead}} - v_{\text{AV}}$.
- $v_{\text{cmd}} : [0, \infty) \rightarrow \mathbb{R}$: speed command for the AV;
- $v_{\text{max}} : [0, \infty) \rightarrow \mathbb{R}$: input to the nominal controller.
- $r : [0, \infty) \rightarrow \mathbb{R}$: reference input to Followerstopper.

When a subscript is not provided in the notation, we mean a generic vehicle. Mathematically, a Followerstopper controller based only on local information can be formulated as

$$v_{\text{cmd}}(t) = f(x_{\text{rel}}(t), v_{\text{rel}}(t), v_{\text{lead}}(t); r) \quad (1)$$

Further, it should also be noted that we use synonymous terms interchangeably, such as traffic waves, shock waves, phantom traffic jams, stop-and-go waves, etc. Similarly, wave-dampening controller, traffic decongestion controller, and traffic smoothing controller refers to the controller for an AV whose goal is to smoothen out the traffic flow over a finite time period.

2.1 Phase-space Design

The control dynamics of Followerstopper controller use a second-order kinematic model. For the longitudinal traffic model shown in Figure 1, the relative distance-relative velocity phase-space ($x_{\text{rel}}-v_{\text{rel}}$ phase-space) falls into three distinct category:

1. A constant relative velocity, i.e. $\frac{dv}{dt} = 0$.
2. A linear relationship between relative distance spacing and relative velocity, i.e. $v_{\text{rel}} = kx_{\text{rel}}$
3. A constant acceleration dynamics.

A phase-space portrait of all three categories is shown in Figure 2.

We model our autonomous car-following controller for the ego vehicle based on the constant acceleration dynamics, which provides a parabolic phase-space trajectory. We have the following kinematic equation for the dynamical system of the third category:

$$v_i(t) = v_{0i}(t) + \alpha_i t \quad (2)$$

where v_{0i} is the initial velocity, α_i is the acceleration of i^{th} vehicle and t is the time-elapsed. The relative velocity between two vehicles can be written as

$$v_{i-1}(t) - v_i(t) = v_{\text{rel}}(t) = v_{\text{rel}0} + (\alpha_{i-1} - \alpha_i)t \quad (3)$$

where $i-1$ indicates the index for the lead vehicle and i is the index for the ego vehicle. Noting $v_{\text{rel}}(t)$ as $\frac{dx}{dt}$, if we consider ω , some specified distance as a design parameter, then we can integrate (3) within the limits $x = \omega$ to $x = x_{\text{rel}}$ from $t = 0$ to $t = t$ as follows:

$$\begin{aligned} \int_{\omega}^{x_{\text{rel}}} dx &= v_{\text{rel}0} \int dt + (\alpha_{i-1} - \alpha_i) \int t dt \\ x_{\text{rel}} - \omega &= v_{\text{rel}0}t + (\alpha_{i-1} - \alpha_i) \frac{t^2}{2} \\ x_{\text{rel}}(t) &= \omega + v_{\text{rel}0}t + (\alpha_{i-1} - \alpha_i) \frac{t^2}{2} \end{aligned} \quad (4)$$

Using t from (3), we can write (4) as :

$$x_{\text{rel}}(t) = \omega + v_{\text{rel}0} \frac{v_{\text{rel}}(t) - v_{\text{rel}0}}{(\alpha_{i-1} - \alpha_i)} + \frac{1}{2} \frac{(v_{\text{rel}}(t) - v_{\text{rel}0})^2}{(\alpha_{i-1} - \alpha_i)} \quad (5)$$

If the vehicles start from rest with the same initial velocity, i.e., $v_{\text{rel}0} = 0$, then

$$x_{\text{rel}}(t) = \omega + \frac{v_{\text{rel}}(t)^2}{2\alpha} \quad (6)$$

with $\alpha = \alpha_{i-1} - \alpha_i$ as another design parameter. A representative phase-portrait corresponding to Equation (6) is provided in Figure 3. Vectors denoted by arrows on the phase-portrait pointing downward/leftward indicate rapid closure of gaps. The gray dashed line marks the desired minimal spacing.

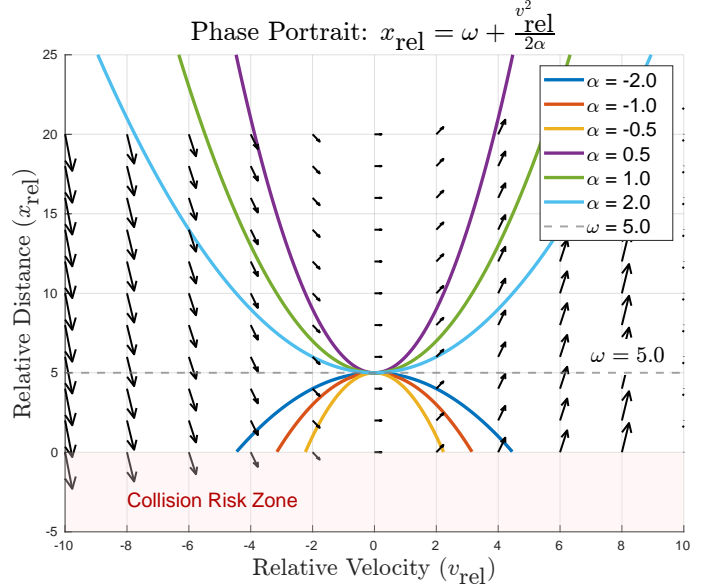


Figure 3: Phase-Space Portraits for $x_{\text{rel}}-v_{\text{rel}}$ with a fixed $\omega = 5$ and varying α . Vectors in the region pointing downward/leftward indicate rapid closure of the gap between the leader and the ego vehicle. Quiver plot is shown for $\alpha = 1$.

ing. Trajectories crossing this line indicate transitions between safe/unsafe states. Further, $\alpha > 0$

In the case of a leader-follower scenario, the negative relative velocity of the leader with respect to the ego vehicle indicates that the ego vehicle is falling behind. In such a case, the controller should command the ego vehicle with velocity $u = v_{i-1}$ to close the gap. Therefore, we modify the phase-space equation as

$$x_{\text{rel}}(t) = \omega + \frac{1}{2\alpha} (\min\{0, v_{\text{rel}}(t)\})^2 \quad (7)$$

A modified phase-portrait corresponding to Equation (7) is presented in Figure 4.

3 Followerstopper: Non-linear Controller for Wave Dampening

In order to dampen the traffic waves arising as a result of the bottleneck, the velocity controller of the form provided in Equation (1) needs to modulate the speed of AV to close the gap between the leader and the ego gracefully so that acceleration or deceleration doesn't amplify the traffic waves along with staying at the safe distance from the leader vehicle. The control law is defined as follows:

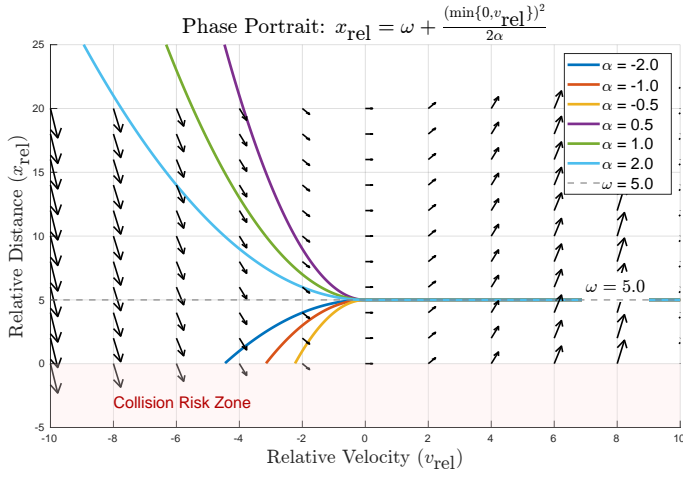


Figure 4: Phase-Space Portraits for $x_{\text{rel}}-v_{\text{rel}}$ with a fixed $\omega = 5$ and varying α for Equation (7).

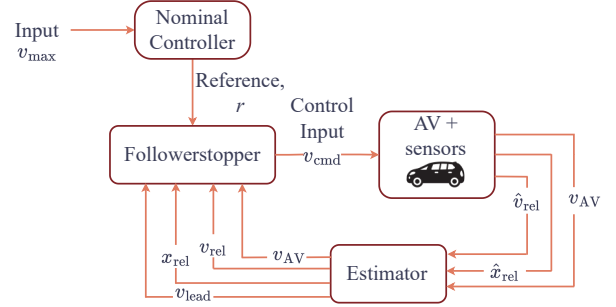


Figure 5: A schematic diagram of Followerstopper controller and other components used for the AV control.

$$f_{\text{FS}}(x_{\text{rel}}(t), v_{\text{rel}}(t), v_{\text{lead}}(t)) = \begin{cases} 0, & \text{if } (x_{\text{rel}}, v_{\text{rel}}) \in \mathcal{S}_1 \\ v(v_{\text{lead}}) \frac{x_{\text{rel}} - d_1(t)}{d_2(t) - d_1(t)}, & \text{if } (x_{\text{rel}}, v_{\text{rel}}) \in \mathcal{S}_2 \\ v(v_{\text{lead}}) + (r - v(v_{\text{lead}})) \frac{x_{\text{rel}} - d_2(t)}{d_3(t) - d_2(t)}, & \text{if } (x_{\text{rel}}, v_{\text{rel}}) \in \mathcal{S}_3 \\ r, & \text{if } (x_{\text{rel}}, v_{\text{rel}}) \in \mathcal{S}_4 \end{cases} \quad (8)$$

where $v : \mathbb{R} \rightarrow \mathbb{R}$ is $v(v_{\text{lead}}) = \min\{\max\{v_{\text{lead}}, 0\}, r\}$. Four sets $\mathcal{S}_1, \mathcal{S}_2, \mathcal{S}_3$, and \mathcal{S}_4 divided by three safety envelopes as are defined below:

$$\begin{aligned} \mathcal{S}_1 &= \{(x_{\text{rel}}, v_{\text{rel}}) \in \mathbb{R}^2 \mid 0 \leq x_{\text{rel}} \leq d_1(v_{\text{rel}})\}, \\ \mathcal{S}_2 &= \{(x_{\text{rel}}, v_{\text{rel}}) \in \mathbb{R}^2 \mid d_1(v_{\text{rel}}) < x_{\text{rel}} \leq d_2(v_{\text{rel}})\}, \\ \mathcal{S}_3 &= \{(x_{\text{rel}}, v_{\text{rel}}) \in \mathbb{R}^2 \mid d_2(v_{\text{rel}}) < x_{\text{rel}} \leq d_3(v_{\text{rel}})\}, \\ \mathcal{S}_4 &= \{(x_{\text{rel}}, v_{\text{rel}}) \in \mathbb{R}^2 \mid d_3(v_{\text{rel}}) < x_{\text{rel}}\}. \end{aligned} \quad (9)$$

The phase-portrait specified in Equation (7) separates switching region with $d_j : \mathbb{R} \rightarrow \mathbb{R}$ are:

$$d_j(v_{\text{rel}}) = \omega_j + \frac{1}{2\alpha_j} \min\{0, v_{\text{rel}}\}^2, \quad j = 1, 2, 3, \quad (10)$$

where $\omega_1 = 4.5$, $\omega_2 = 5.25$, $\omega_3 = 6.0$, $\alpha_1 = 1.5$, $\alpha_2 = 1$, $\alpha_3 = 0.5$. Through our controller design, we control the velocity of the Lagrangian control vehicle (ego vehicle), through the control input u as shown in 5.

The switching region as specified by Equation (10) is illustrated in Figure 6.

3.1 Nominal Controller

The overall structure of the controller, as illustrated in Figure 5, shows that it requires an input speed that serves as a basis for

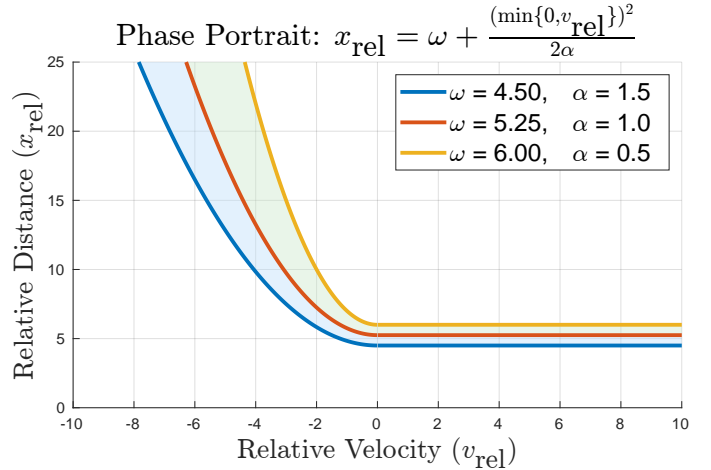


Figure 6: Switching regions allows a smoother transition from speeding up to catch up to the lead vehicle, to decelerating to match the lead vehicle's velocity, to braking to avoid an impending collision.

the reference speed to the AV. However, to constrain the input within the bounds of physics so as not to cause any abrupt acceleration or deceleration (or example, at one time-step if the input is velocity of $4m/s$ and then in the next time step it is $12.0m/s$), the nominal controller further modulates the reference speed before feeding it into Followerstopper. The algorithm used for the nominal control is specified in Algorithm 1.

Algorithm 1 Nominal Control Reference Velocity Calculation

Require: max_speed : Desired velocity (m/s), vel : Current velocity (m/s), max_accel : Maximum acceleration (m/s^2), max_decel : Maximum deceleration (m/s^2)

Ensure: r : Reference velocity for Followerstopper controller (m/s)

```

1:  $persistent\ y \leftarrow 0$  ▷ Initialize internal state variable
2:  $dt \leftarrow 0.05$  ▷ Time step (s)
3: if  $y\ max\_speed + 1$  then
4:    $y \leftarrow \max(max\_speed, y - |max\_decel| \cdot dt)$ 
5: else if  $y\ max\_speed - 1$  then
6:    $y \leftarrow \min(max\_speed, y + max\_accel \cdot dt)$ 
7: else
8:    $y \leftarrow max\_speed$  ▷ Maintain target speed
9: end if
10: if  $y\ 2$  and  $max\_speed\ 2$  then ▷ Speed floor constraints
11:    $y \leftarrow 2$ 
12: else if  $y\ 1$  and  $max\_speed\ 1$  then
13:    $y \leftarrow 1$ 
14: end if
15:  $r \leftarrow \min(\max(y, vel - 1.0), vel + 2.0)$  ▷ Output smoothing
16: return  $r$ 
```

3.2 Implementation Details

We used MATLAB's Robot Operating System (ROS) Toolbox [22] and Simulink to implement Followerstopper defined in Equation (8). The ego vehicle used for our experiment was the University of Arizona's CAT Vehicle that uses ROS for high-level control and at a lower level, a ROS2JAUS interface [23] sends a command to the vehicle's actuator. Using ROS Toolbox from Simulink, we were able to generate native ROS code to transfer to CAT Vehicle's hardware. A snapshot of Simulink blocks to implement Followerstopper and Nominal Controller is provided in Figure 7 and Figure 8, respectively.

4 Results

While the overall result of the Arizona-ring Road Experiment, where Followerstopper controller was tested, is available in [15], we briefly present the time-space diagram of the experiment in Figure 9 for the sake of completeness. The time-space diagram shows the formation of stop-and-go waves at around $t = 79$ s. At $t = 126$ s from the experiment, we activated the autonomous mode of CAT Vehicle, and Followerstopper took over the control of the vehicle. At this point, user-specified input for max speed, as the input to the Nominal Controller, was $6.5m/s$, which was provided by an expert human observing the ring traffic from a bird-eye view. It took approximately 30-35 seconds before we could observe the im-

pact of Followerstopper's wave-dampening capability. For the next several minutes, we varied the user-specified reference velocity to assess the impact of the reference velocity setpoint on the ring traffic. A list of various reference velocity setpoints used during the experiment is shown in Table 1. We observed the best performance of the wave-dampening effect at the reference speed of $7.5m/s$.

| Time into the Experiment | Reference Velocity |
|--------------------------|--------------------|
| 0–126 s | Manual driving |
| 126–222 s | 6.5 m/s |
| 222–292 s | 7.0 m/s |
| 292–347 s | 7.5 m/s |
| 347–415 s | 8.0 m/s |
| 415–463 s | 7.5 m/s |
| 463 s | Manual driving |

Table 1: Varying reference velocity for different time intervals specified during the Arizona ring-road experiment to demonstrate the wave-dampening capability of Followerstopper

We also provide $x_{rel} - v_{rel}$ phase-space diagram for the AV in Figure 10. We see that the phase-space curve is not seen in the Collision Risk Zone when the autonomous mode was active under Followerstopper control. Thus, we conclude that for the speed regime under which the autonomous vehicle was operating, its behavior was safe.

5 Data and Code Availability

Data generated as a part of Arizona Ring-road Experiment is available at <http://hdl.handle.net/1803/9358>. Code used to generate figures along with Simulink models of Followerstopper are available on <https://github.com/AARC-lab/Followerstopper>. Appendix A provides m-file implementations of Followerstopper and Nominal controller algorithm (provided as smoothUpParams function).

6 Conclusion and Future Work

In this paper, we provided the mathematical derivation and complete formulation of Followerstopper controller that demonstrated its ability to dampen stop-and-go traffic waves in the Arizona Ring-road Experiment. The nominal controller that regulates the reference input to Followerstopper was formally presented for the first time, addressing a gap in the literature.

A natural extension of Followerstopper can utilize a control barrier certificate, as Equation (10) acts as a barrier function. The work presented in this manuscript can be extended to take into account uncertainty in state estimation to evaluate controller stability and modify its formulation.

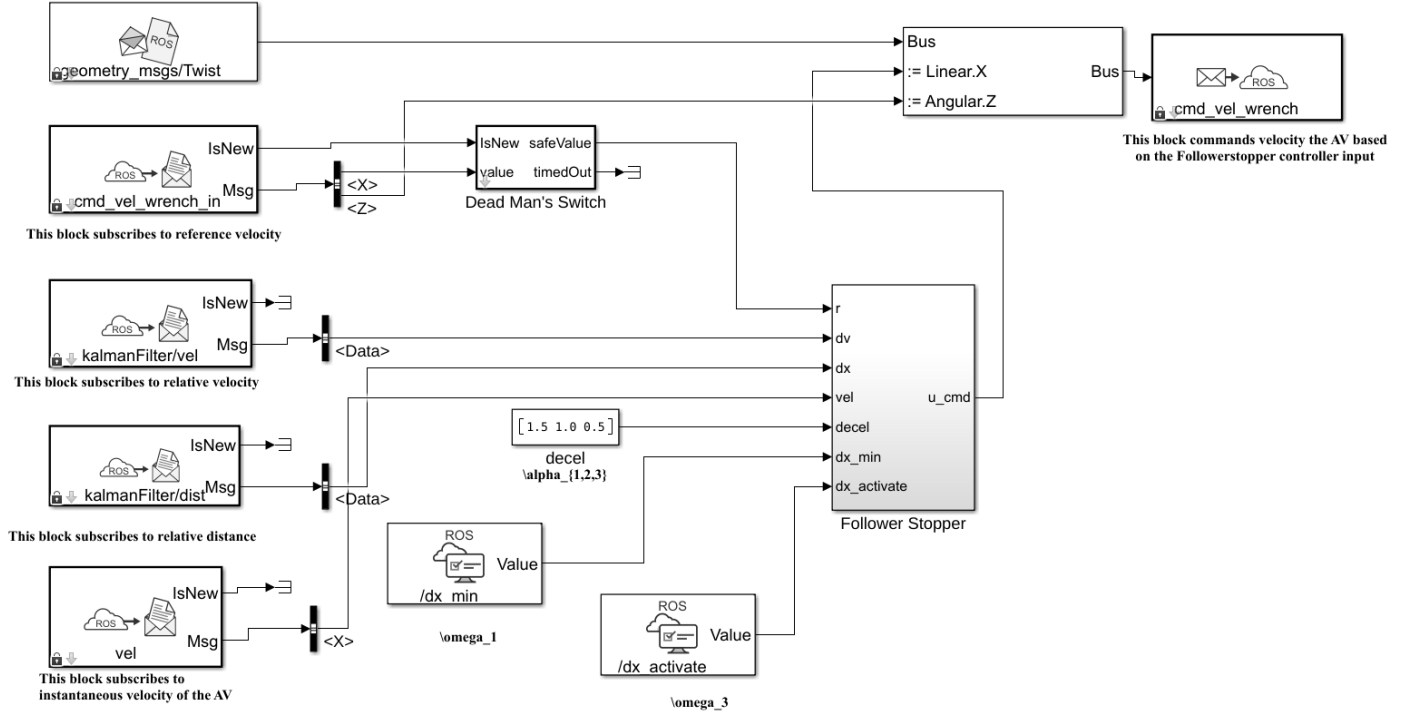


Figure 7: Followerstopper Simulink Model. The function block specifies the logic from Equation (8).

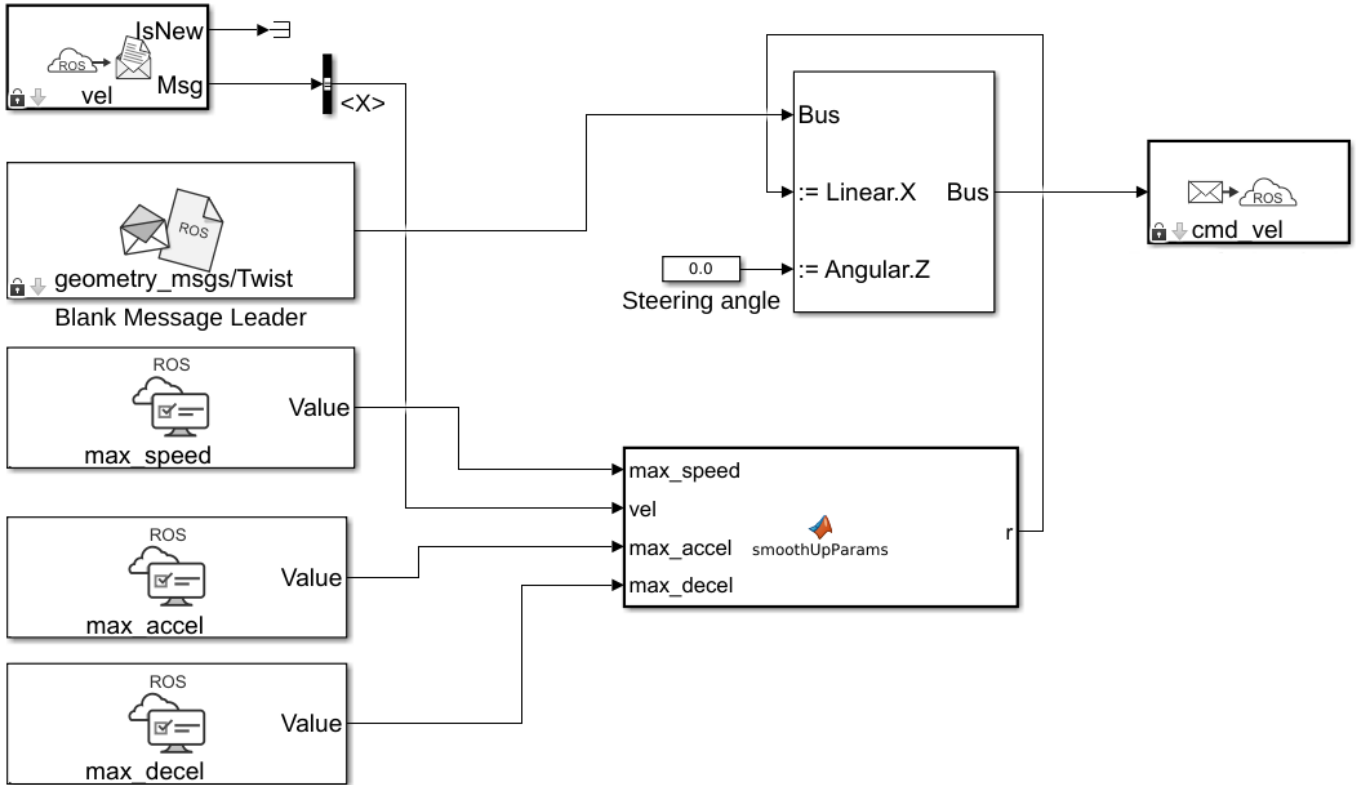


Figure 8: Nominal Controller Implementation in smoothUpParams Simulink Block as specified in Algorithm 1. cmd_vel publisher block is mapped to cmd_vel_wrench_in subscriber block from Followerstopper Simulink Model shown in Figure 7.

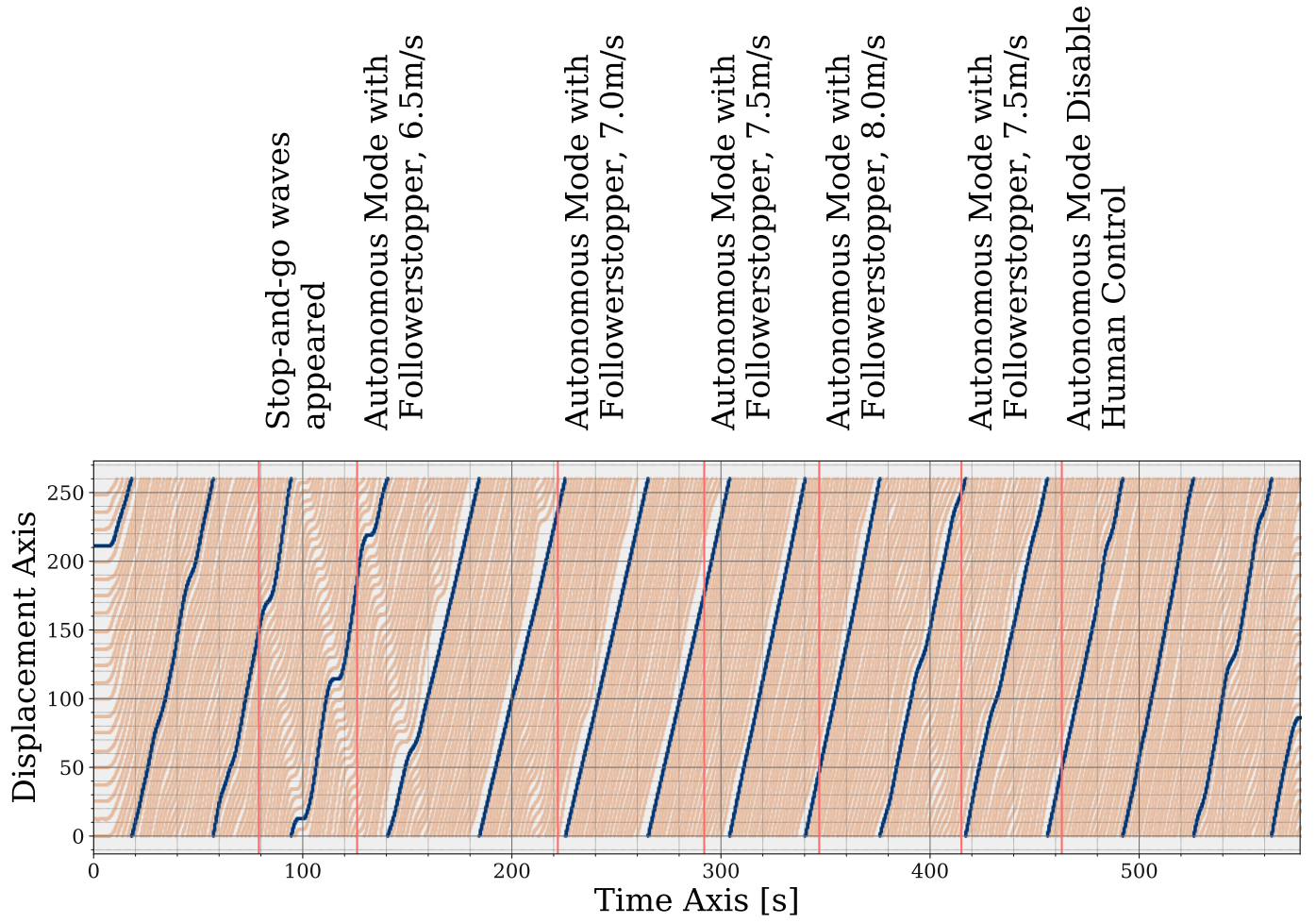


Figure 9: Annotated time-space diagram for Arizona-ring road experiment with Followerstopper's wave-dampening capability.

$x_{rel}v_{rel}$ phase space evolution
when different input to the Nominal Controller

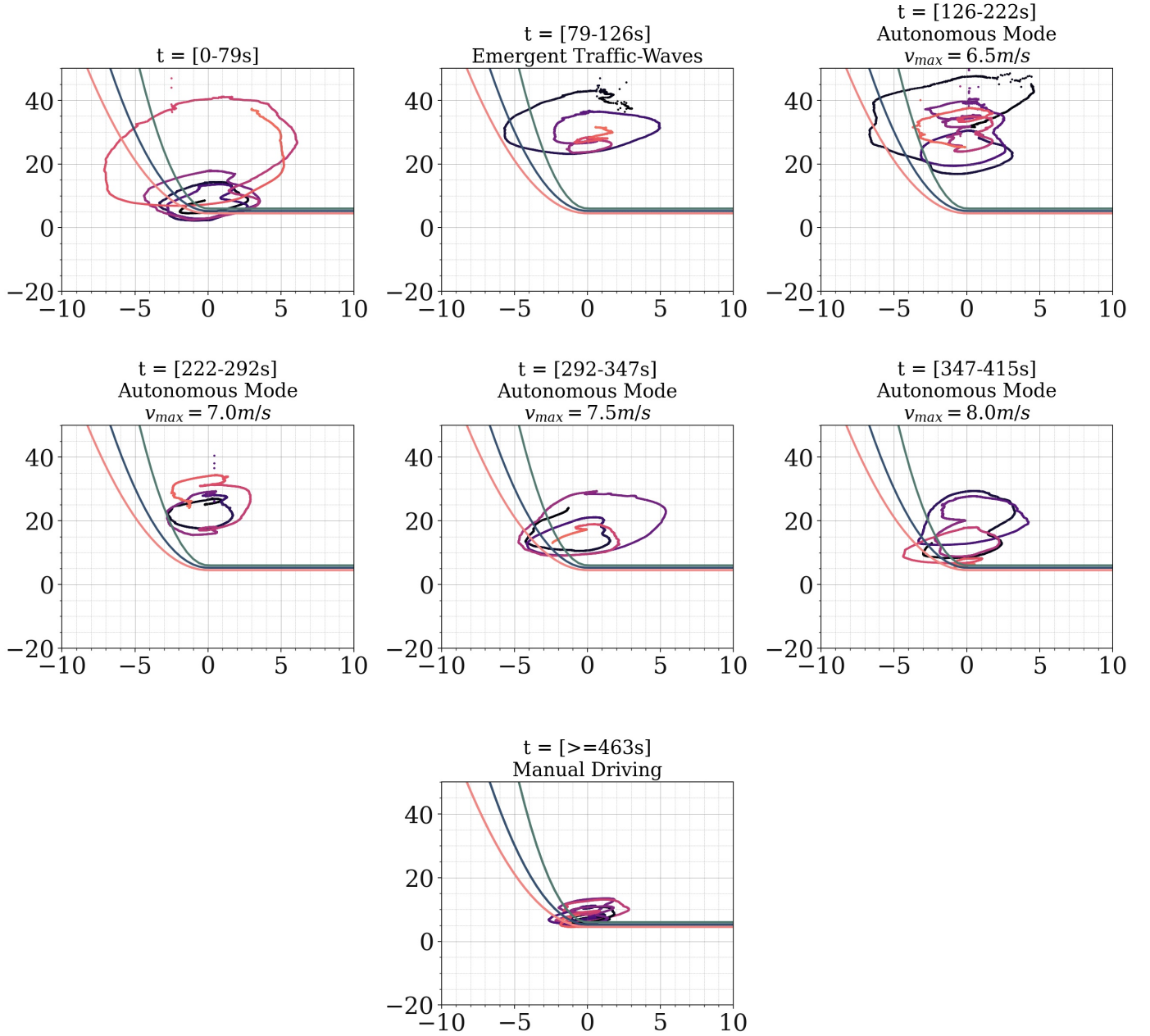


Figure 10: $x_{rel} - v_{rel}$ evolution overlaid with the switching boundary.

References

- [1] Y. S. Chang, Y. J. Lee, and S. S. B. Choi, "Is there more traffic congestion in larger cities?-scaling analysis of the 101 largest us urban centers," *Transport Policy*, vol. 59, pp. 54–63, 2017.
- [2] M. Saberi, H. Hamedmoghadam, M. Ashfaq, S. A. Hosseini, Z. Gu, S. Shafiei, D. J. Nair, V. Dixit, L. Gardner, S. T. Waller *et al.*, "A simple contagion process describes spreading of traffic jams in urban networks," *Nature communications*, vol. 11, no. 1, pp. 1–9, 2020.
- [3] S. Çolak, A. Lima, and M. C. González, "Understanding congested travel in urban areas," *Nature communications*, vol. 7, no. 1, pp. 1–8, 2016.
- [4] D. Helbing, "Traffic and related self-driven many-particle systems," *Reviews of modern physics*, vol. 73, no. 4, p. 1067, 2001.
- [5] E. Chevallier, A. Can, M. Nadji, and L. Leclercq, "Improving noise assessment at intersections by modeling traffic dynamics," *Transportation Research Part D: Transport and Environment*, vol. 14, no. 2, pp. 100–110, 2009.
- [6] S. Ossen and S. P. Hoogendoorn, "Driver heterogeneity in car following and its impact on modeling traffic dynamics," *Transportation research record*, vol. 1999, no. 1, pp. 95–103, 2007.
- [7] D. H. Nam and D. R. Drew, "Analyzing freeway traffic under congestion: Traffic dynamics approach," *Journal of Transportation Engineering*, vol. 124, no. 3, pp. 208–212, 1998.
- [8] P. G. Gipps *et al.*, "Behavioral car-following model for computer simulation," *Transport. Res.*, vol. 15, no. 2, pp. 105–111, 1981.
- [9] H. Ge, S. Dai, L. Dong, and Y. Xue, "Stabilization effect of traffic flow in an extended car-following model based on an intelligent transportation system application," *Physical Review E*, vol. 70, no. 6, p. 066134, 2004.
- [10] R. F. Benekohal and J. Treiterer, "Carsim: Car-following model for simulation of traffic in normal and stop-and-go conditions," *Transportation research record*, vol. 1194, pp. 99–111, 1988.
- [11] T. Tang, Y. Wang, X. Yang, and Y. Wu, "A new car-following model accounting for varying road condition," *Nonlinear Dynamics*, vol. 70, no. 2, pp. 1397–1405, 2012.
- [12] H. Lazar, K. Rhoulami, and D. Rahmani, "A review analysis of optimal velocity models," *Periodica Polytechnica Transportation Engineering*, vol. 44, no. 2, pp. 123–131, 2016.
- [13] Y. Sugiyama, M. Fukui, M. Kikuchi, K. Hasebe, A. Nakayama, K. Nishinari, S.-i. Tadaki, and S. Yukawa, "Traffic jams without bottlenecks—experimental evidence for the physical mechanism of the formation of a jam," *New journal of physics*, vol. 10, no. 3, p. 033001, 2008.
- [14] L. Li, J. Song, F.-Y. Wang, W. Niehsen, and N.-N. Zheng, "Ivs 05: New developments and research trends for intelligent vehicles," *IEEE Intelligent Systems*, vol. 20, no. 4, pp. 10–14, 2005.
- [15] R. E. Stern, S. Cui, M. L. Delle Monache, R. Bhadani, M. Bunting, M. Churchill, N. Hamilton, R. Haulcy, H. Pohlmann, F. Wu *et al.*, "Dissipation of stop-and-go waves via control of autonomous vehicles: Field experiments," *Transportation research part C: emerging technologies*, vol. 89, pp. 205–221, 2018.
- [16] J. Wang, Y. Zheng, Q. Xu, J. Wang, and K. Li, "Controllability analysis and optimal control of mixed traffic flow with human-driven and autonomous vehicles," *IEEE Transactions on Intelligent Transportation Systems*, vol. 22, no. 12, pp. 7445–7459, 2020.
- [17] M. Shang, S. Wang, T. Li, and R. Stern, "Interaction-aware model predictive control for automated vehicles in mixed-autonomy traffic," in *2024 IEEE Intelligent Vehicles Symposium (IV)*. IEEE, 2024, pp. 317–322.
- [18] Y. Wang, Y. Jiang, Y. Wu, and Z. Yao, "Mitigating traffic oscillation through control of connected automated vehicles: A cellular automata simulation," *Expert Systems with Applications*, vol. 235, p. 121275, 2024.
- [19] E. Vinitsky, A. Kreidieh, L. Le Flem, N. Kheterpal, K. Jang, C. Wu, F. Wu, R. Liaw, E. Liang, and A. M. Bayen, "Benchmarks for reinforcement learning in mixed-autonomy traffic," in *Conference on robot learning*. PMLR, 2018, pp. 399–409.
- [20] N. Lichtlé, E. Vinitsky, G. Gunter, A. Velu, and A. M. Bayen, "Fuel consumption reduction of multi-lane road networks using decentralized mixed-autonomy control," in *2021 IEEE International Intelligent Transportation Systems Conference (ITSC)*. IEEE, 2021, pp. 2068–2073.
- [21] A. R. Kreidieh, Z. Fu, and A. M. Bayen, "Learning energy-efficient driving behaviors by imitating experts," in *2022 IEEE 25th International Conference on Intelligent Transportation Systems (ITSC)*. IEEE, 2022, pp. 2689–2695.
- [22] M. Quigley, K. Conley, B. Gerkey, J. Faust, T. Foote, J. Leibs, R. Wheeler, A. Y. Ng *et al.*, "Ros: an open-source robot operating system," in *ICRA workshop on open source software*, vol. 3, no. 3.2. Kobe, 2009, p. 5.
- [23] P. Morley, A. Warren, E. Rabb, S. Whitsitt, M. Bunting, and J. Sprinkle, "Generating a ros/jaus bridge for an autonomous ground vehicle," in *Proceedings of the 2013 ACM workshop on Domain-specific modeling*, 2013, pp. 13–18.

A Simulink Models and Code

A.1 m-file Implementation of Followerstopper

Followertopper Controller

```
1 function u_cmd = FollowerStopper(r,dx,dv,v_AV, dx_min,dx_activate,decel)
2 %#codegen
3 % Safety controller, based on quadratic bands.
4 % Input: r = desired velocity (from other models)
5 %         dx = estimate of gap to vehicle ahead
6 %         dv = estimate of time derivative of dx (= velocity difference)
7 %         v_AV = velocity of AV
8 %         dx_min = minimum distance (omega_1)
9 %         dx_activate = distance below which controller does something (omega_3)
10 %         decel = vector of three deceleration values for parabolas
11 % Out: u_cmd = actual velocity commanded (always u_cmd<=U)
12 %
13 % Controller-specific parameters
14 dx_mid = (dx_min+dx_activate)/2; % mid distance, where v_lead is commanded
15 % Lead vehicle velocity
16 v_lead = v_AV+dv; % velocity of lead vehicle
17 v_lead = max(v_lead,0); % lead vehicle cannot go backwards
18 v = min(r,v_lead); % safety velocity cannot exceed desired velocity U
19 % Treatment of positive dv-values
20 dv = min(dv,0); % domains for dv>0 same as dv=0
21 % For given dv, dx-values of band boundaries
22 dx1 = dx_min+1/(2*decel(1))*dv.^2;
23 dx2 = dx_mid+1/(2*decel(2))*dv.^2;
24 dx3 = dx_activate+1/(2*decel(3))*dv.^2;
25 % Actual commanded velocity
26 u_cmd = double((dx1<dx&dx<=dx2).*(v.*(dx-dx1)./(dx2-dx1))+...
27             (dx2<dx&dx<=dx3).*(v+(r-v).*(dx-dx2)./(dx3-dx2))+...
28             (dx3<dx).*r);
29
30 if( dx > 16.0 )
31     u_cmd = r;
32 end
```

A.2 m-file Implementation of Nominal Controller

Nominal Controller

```
1 function r = smoothUpParams(max_speed,vel,max_accel,max_decel)
2 %#codegen
3 % Input: max_speed = desired velocity from user
4 %         vel = current velocity of the vehicle
5 %         max_accel = maximum permissible acceleration
6 %         max_decel = maximum permissible deceleration
7 %         dx_min = minimum distance (omega_1)
8 %         dx_activate = distance below which controller does something (omega_3)
9 %         decel = vector of three deceleration values for parabolas
10 % Out: r =reference velocity to the Followerstopper
11
12 persistent y
13
14 if isempty(y)
15     y=0;
16 end
17
18 dt=0.05;
19 if( y > max_speed + 1 )
20     y = max(max_speed,y - abs(max_decel)*dt);
21 elseif( y < max_speed - 1)
22     y = min(max_speed,y + max_accel*dt);
23 else
24     y = double(max_speed);
25 end
26
27 if (y < 2 && max_speed > 2)
28     y = 2;
29 elseif(y < 1 && max_speed > 1)
30     y = 1;
31 end
32
33 r =min(max(y,vel-1.0),vel+2.0);
```